Appl. Phys. 15, 119—131 (1978)

Applied Physics

Optical Ramsey Fringes in Two-Photon Spectroscopy*

*M. M. Salour***

Department of Physics and Gordon McKay Laboratory, Harvard University, Cambridge, MA 02138, USA

Received 11 August 1977/Accepted 30 October 1977

Abstract. Using two coherent time delayed short pulses, we have demonstrated that one can obtain, in the profile of Doppler-free two-photon resonances, interference fringes with a splitting $1/2\,T$ (T: delay time between the two pulses) much smaller than the spectral width $1/\tau$ of each pulse (τ: duration of each pulse). Furthermore, by inducing a 90° phase shift between pairs of coherent time-delayed laser pulses, and subtracting the resulting fluorescence from pairs of coherent pulses with and without the phase shift, we have eliminated the diffraction background and isolated the Ramsey's interference fringes in the profile of Doppler-free two-photon resonances. This technique should lead to a number of important improvements in the presently available methods of ultra-high resolution laser spectroscopy of atoms, molecules, and crystals.

PACS: 07.65

Interaction of atoms and molecules with intense monochromatic laser standing waves can give rise to very narrow Doppler-free two-photon resonances. This new high resolution spectroscopic method has recently been extensively applied to the study of several atomic and molecular optical transitions [1]. The discovery and accurate measurement of these narrow, frequency-stable resonance lines in the emission and absorption spectra of substances are significant because advances in this area will not only provide direct clues to the innermost processes of matter, but may also lead to novel applications in many areas of science.

The ultimate resolution achievable by the method of Doppler-free two-photon spectroscopy is limited in principle only by the natural linewidth of the excited state; in practice, however, the observed linewidth has thus far been limited by the laser. Thus in order to take full advantage of the elimination of the Doppler width, the spectral linewidth of the laser light must be as small as possible, which explains the motivation for using cw lasers. But, on the other hand, two-photon resonances require an appreciable power, and it is well known that pulsed dye lasers[1] deliver higher powers and, furthermore, cover a broader spectral range. Recently, by using pulsed dye lasers pumped with an N_2 laser, it has been possible to observe two-photon resonances in several highly excited states of various atomic vapors which could not have been reached by cw excitation [2]. The resolution was limited by the spectral width $1/\tau$ of the pulse (τ: duration of each pulse), thus making it impossible to resolve many closely spaced two-photon resonance lines.

In this paper, we will demonstrate that, by exciting atoms with two time-delayed coherent laser pulses, one can obtain interference fringes in the profile of the Doppler-free two-photon resonances with a splitting $1/T$ (T: delay between the two pulses) much smaller than the spectral width $1/\tau$ (τ: duration of each pulse). This technique combines the advantages of pulsed dye lasers (power, spectral range) with the high resolution usually associated with a cw excitation. Our experiment can be considered as an extension to two-photon Doppler-free resonances in the optical range of the well-known Ramsey method of using two separated RF or microwave fields in atomic beam experiments [3].

Such an idea was first suggested in a slightly different context by Baklanov et al. [4], who proposed using two spatially separated cw light standing waves to study new physical features involving the nonlinear interaction of an atomic ensemble with widely separated

* Supported in part by the Joint Services Electronics Program.

** Present address: Optics Section, Dept. of Physics, Imperial College, London SW 7 2BZ, England.

[1] For details the reader is referred to [11, 12].

0340-3793/78/0015/0119/$02.60

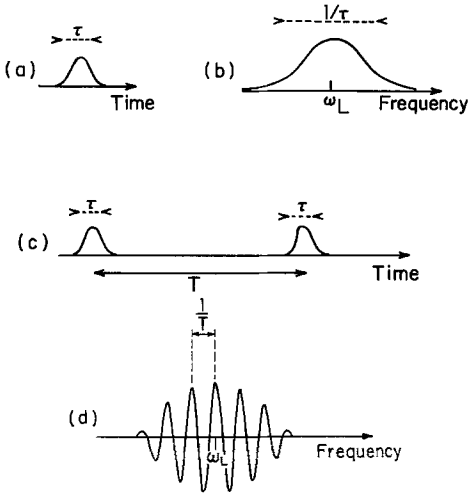

Fig. 1a—d. Single and time-delayed pulses and frequency patterns

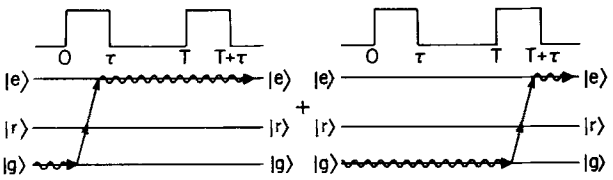

Fig. 2. Two quantum mechanical amplitudes contributing the total amplitude to order E^2

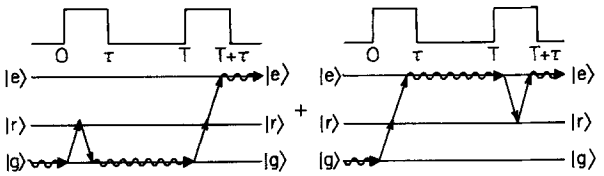

Fig. 3. Two quantum mechanical amplitudes contributing to the total amplitude to order E^4

optical fields. These authors considered two-photon Doppler-free resonances between two very sharp levels, such as ground states or metastable states (an important example being the $1S_{1/2}-2S_{1/2}$ transition of H). In such a case, the use of a single laser beam leads to linewidths which are generally limited by the inverse of the transit time of atoms through the laser beam. Rather than increasing this time by expanding the laser beam diameter (with a consequent loss of intensity), Baklanov et al. proposed using two spatially separated beams to obtain structures in the profile of the resonance having a width determined by the time of flight between the two beams. (Similar optical Ramsey fringes have recently been observed by Bergquist et al. [5] in saturated absorption spectroscopy of a beam of fast neon atoms with spatially separated laser fields.) The experiment described below deals with short-lived atomic states (lifetime $\sim 5\times 10^{-8}$ s), so that the transit time through the laser beam ($\sim 10^{-7}$ s) plays no role in the problem. Consequently, we use two time-delayed short pulses instead of two spatially separated beams [6].

The interference structure appearing in the resonance profile can be simply understood in the following way. Consider first a single pulse of the form $E(t)\exp(-i\omega t)$, where the envelope function $E(t)$ has the shape represented in Fig. 1a (τ: duration of the pulse). The Fourier analysis of such a pulse leads to a frequency spectrum spread over an interval $1/\tau$ around ω (Fig. 1b). This nonmonochromatic excitation acting upon the atom leads to a Doppler-free two-photon resonance having a width $1/\tau$. Suppose now that $E(t)$ has the shape represented in Fig. 1c (two pulses of duration τ separated by a delay T). Just as the diffraction pattern through two spatially separated slits exhibits interference fringes within the diffraction profile corresponding to a single slit, the Fourier transform of the electric field corresponding to Fig. 1c exhibits interference fringes within the spectrum profile of a single pulse (Fig. 1d), with a frequency splitting of $1/T$ between two fringes.

1. Formalism

Two important requirements must be fulfilled in order to obtain such interference fringes in the profile of the two-photon resonance. First, each pulse must be reflected against a mirror placed near the atomic cell in order to expose the atoms to a pulsed standing wave and in this way to suppress any dephasing factor due to the motion of the atoms. The probability amplitude for absorbing two counterpropagating photons is proportional to $\exp[i(\omega t-kz)]\exp[i(\omega t+kz)]=\exp(2i\omega t)$ and does not depend on the spatial position z of the atoms. Second, the phase difference between the two pulses must remain constant during the entire experiment. Significant phase fluctuations between the two pulses will wash out the interference fringes, since any phase variation produces a shift of the whole interference structure within the diffraction background. To avoid such fluctuations, the experiment must be done not with two independent pulses, but with two time-delayed pulses having a constant phase difference during the entire experiment. Furthermore, these two pulses have to be Fourier limited, that is, their coherence times must be not shorter than their durations.

From a more physical point of view, one can think of a two-level system, $|g\rangle$ and $|e\rangle$. After the first pulse the atomic state is a coherent superposition of the two levels. Atoms in this superposition freely precess and, depending on the point in time at which the delayed pulse arrives (while the excited atom is still freely

precessing), one can see either constructive or destructive interference with the precession of the excited atomic state.

Note again that it is important that the initial and the delayed pulses be phase-locked. Otherwise, when the delayed pulse arrives, the random phase difference between initial and delayed pulses will give rise randomly to constructive or destructive interference, and when averaged the interference signal will be washed out.

Yet another interpretation of this interference can be shown diagrammatically:

Figure 2 represents two quantum mechanical amplitudes whose sum represents the total amplitude, of order E^2 (each photon contributes a factor of E), for reaching the excited state $|e\rangle$ from the ground state $|g\rangle$. The probability of reaching the $|e\rangle$ state is then the absolute square of this sum, and the cross term appearing in this absolute square represents the interference signal.

Higher-order processes can also become important, especially at higher laser intensities. Figure 3 illustrates additional amplitudes of order E^4 which contribute to the interference signal. These diagrams have the physical interpretation of ac Stark shift of the $|g\rangle$ and $|e\rangle$ states via mixing with the intermediate state $|r\rangle$. These processes would result in linear power shift of the interference signal.

The experiments discussed in this paper were all performed on the 3^2S-4^2D two-photon excitation in sodium. Sodium atoms in the 3^2S ground state were excited to the 4^2D state by two photons at 5787.3 Å (Fig. 4), and the resulting fluorescence at 3302 Å was collected by a photomultiplier. The wavelength of this transition (5787.3 Å) falls at the peak of the gainband of the Rhodamine 6 G cw dye laser. Since we wished to employ a cw dye laser oscillator with synchronized pulsed amplifiers in order to obtain a Fourier limited pulse, this transition was clearly a possible choice for our experiment. One other possible choice was the 3^2S-5^2S two-photon transition, whose wavelength (6022.3 Å) also lies in the gain-band of the Rhodamine 6 G cw dye laser, although with less power (almost a factor of three smaller, although various dye mixtures could perhaps substantially increase the gain at 6022 Å). The real advantage of the 3^2S-4^2D transition over the 3^2S-5^2S transition becomes clear, however, when one compares the two-photon transition probabilities for the two transitions. Such comparison [7] reveals that under normal experimental situations the signal would be 50 times stronger for the 4^2D level than for the 5^2S level. More importantly, since the fine structure of the excited 4^2D state of sodium and the hyperfine structure of the ground state are known very accurately, the 4^2D level would allow a more accurate frequency calibration of our data from the reference sodium cell than the 5^2S level.

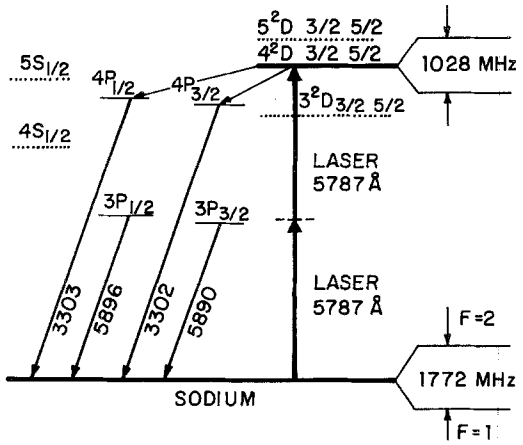

Fig. 4. Energy level diagram of sodium and the two-photon excitation scheme

2. First Possible Experiment

A first possible method for obtaining a sequence of two phase-locked and Fourier limited pulses is to start with the cw dye laser wave of Fig. 5a at frequency ω (having a very long coherence time), and to amplify it with the two time-delayed pulsed-amplifiers of Fig. 5b. Even if the cw laser delivers a very weak intensity in the spectral range under study, with a sufficient number of synchronized pulsed amplifiers one can obtain enough power to observe the two-photon resonance. The time dependence of the amplified wave has the shape represented by the solid lines of Fig. 5c. The two pulses are portions of the same sinusoid (represented in dotted lines), and clearly have the same phase, that of the cw carrier wave. Thus if we neglect the cw background, the electric field that excites atoms may be written

$$E(t)=\begin{cases} E\,e^{-i(\omega t-\phi)} & \text{for } 0\leqq t\leqq\tau \\ E\,e^{-i(\omega t-\phi)} & \text{for } T\leqq t\leqq T+\tau \\ 0 & \text{elsewhere} \end{cases} \tag{1}$$

where τ is the width of each pulse, T is the delay between the two pulses, ω is the cw laser angular frequency, and ϕ is the phase of the cw laser carrier.

It can be shown that the two-photon transition between the ground state $|g\rangle$ and the excited state $|e\rangle$ induced by two counter-propagating waves of amplitude E and frequency ω, for a separation of $\omega_0=2\omega$, is equivalent to the problem of a two-level system $|1\rangle$ and $|2\rangle$, separated by ω_0 (where ω_0 is the Bohr frequency of the atomic transition), with an "effective" dipole moment $\mathscr{D}$, excited by a field $\mathscr{E}\exp[-i(2\omega t-\theta)]$, where $\mathscr{E}$ is proportional to E^2, θ is a phase depending on the mirror reflecting the incident wave, and $\mathscr{D}$ is proportional to

$$\sum_r \frac{\langle e|\boldsymbol{D}|r\rangle\langle r|\boldsymbol{D}|g\rangle}{E_g+\omega-E_r},$$

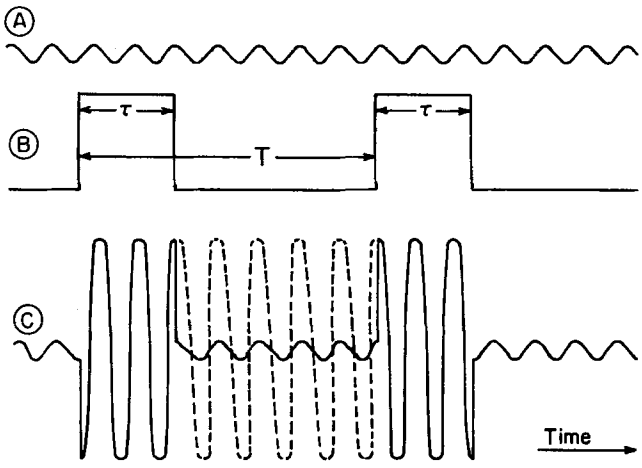

Fig. 5a—c. Pulsed amplification of cw dye laser wave. (a) cw laser wave. (b) Time dependence of amplification. (c) Amplified wave

where $\boldsymbol{D}$ is the atomic dipole moment. (To simplify calculations, we take $\hbar=1$ throughout this paper.)
Again we note that in calculating the probability amplitude for absorbing two counterpropagating photons, the two r-dependent factors [$\exp(i\boldsymbol{k}\cdot\boldsymbol{r})$ and $\exp(-i\boldsymbol{k}\cdot\boldsymbol{r})$] cancel when multiplied. Hence the position $\boldsymbol{r}$ of the atom plays absolutely no role in our problem, and the motion of the atoms causes no dephasing.
Using the Schrödinger equation for this two-level system,

$$|2\rangle \quad \overset{\uparrow}{\underset{\omega_0}{}} \quad |\psi\rangle = a(t)|1\rangle + b(t)|2\rangle \qquad (2)$$
$$|1\rangle \quad \downarrow$$

one finds the equation for the evolution of b

$$i\dot{b} = \omega_0 b - \mathscr{D}\mathscr{E}(t)a. \qquad (3)$$

From the incident wave of Fig. 5c, we can determine the value of $\mathscr{D}\mathscr{E}(t)$ to be

$$-\mathscr{D}\mathscr{E}(t) = \begin{cases} \omega_1 e^{-2i\omega t} & \text{for } 0 \leqq t \leqq \tau \\ \omega_1 e^{-2i\omega t} & \text{for } T \leqq t \leqq T+\tau \\ 0 & \text{elsewhere} \end{cases} \qquad (4)$$

where

$$\omega_1 \sim E^2. \qquad (5)$$

Note that the phases ϕ [appearing in (1)] and θ (appearing in $\exp[-i(2\omega t-\theta)]$ disappear at the end of our calculations, and thus can be taken equal to zero from the beginning.
We can simplify our calculation by going to the interaction representation, taking

$$\left.\begin{aligned} \tilde{a} &= a \\ \tilde{b} &= b\, e^{i\omega_0 t} \end{aligned}\right\}. \qquad (6)$$

Thus from (4) and (5) the Schrödinger equation becomes

$$\left.\begin{aligned} i\dot{\tilde{b}} &= \omega_1 e^{i(\omega_0 - 2\omega)t}\tilde{a} \quad \text{for } 0 \leqq t \leqq \tau \text{ and for } T \leqq t \leqq T+\tau \\ i\dot{\tilde{b}} &= 0 \qquad\qquad\qquad\quad \text{elsewhere} \end{aligned}\right\}. \qquad (7)$$

For the two-photon process we can assume that ω_1 is sufficiently small, and that the duration τ of each pulse is sufficiently short, so that if atoms are in the lower state before the first pulse (i.e., $a=1$ and $b=0$), then $\tilde{b}(t)$ remains very small after each pulse and $\tilde{a}(t)$ is practically equal to one. Consequently, we can replace $\tilde{a}$ by one in (7) and thus obtain

$$\left.\begin{aligned} i\dot{\tilde{b}} &= \omega_1 e^{i(\omega_0 - 2\omega)t} \quad \text{for } 0 \leqq t \leqq \tau \text{ and for } T \leqq t \leqq T+\tau \\ i\dot{\tilde{b}} &= 0 \qquad\qquad\qquad\quad \text{elsewhere} \end{aligned}\right\}. \qquad (8)$$

It is possible to perform the calculations for any value of ω_1 and τ by using the rotating frame representation rather than the interaction representation, of course. But the perturbative calculation presented here is much simpler and contains the main physical ideas.
In order to find the state of the atom after the first pulse, we integrate (8) between zero and τ with the initial condition $\tilde{b}(0)=0$. We obtain the probability amplitude $b_1=\tilde{b}(\tau)$ for finding the atom in the upper state immediately after the first pulse

$$b_1 = \tilde{b}(\tau) = -\frac{\omega_1}{\omega_0 - 2\omega}\left[e^{i(\omega_0 - 2\omega)\tau} - 1\right]. \qquad (9)$$

Note that according to (8), $\tilde{b}(t)$ does not change between the two pulses, but remains equal to b_1. (For the time

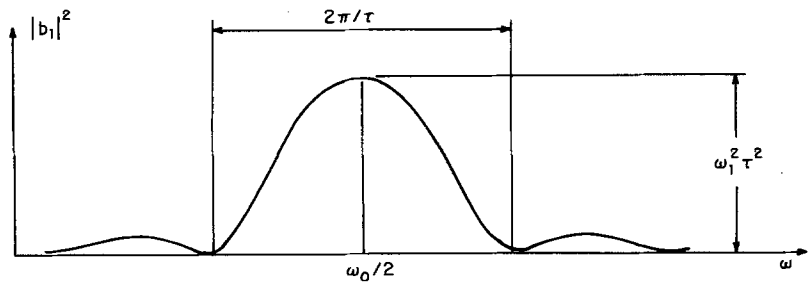

Fig. 6. $|b_1|^2$ as a function of the laser angular frequency ω

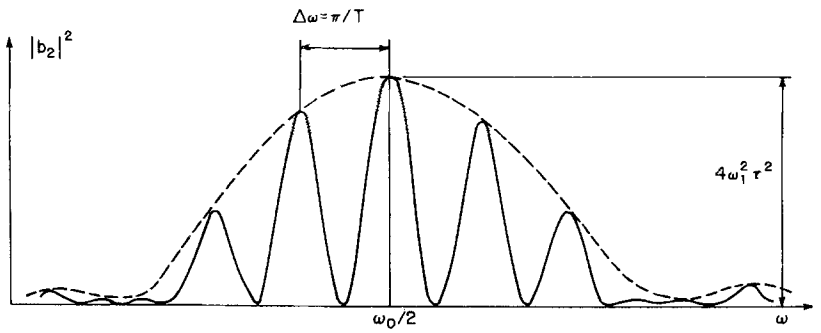

Fig. 7. $|b_2|^2$ as a function of the laser angular frequency ω

being we have neglected the damping due to spontaneous emission. We will take it into account later.) Therefore, by integrating (8) between T and $T+\tau$ with initial condition $\tilde{b}(T)=b_1$, we obtain the probability amplitude $b_2=\tilde{b}(T+\tau)$ for finding the atom in the upper state after the second pulse

$$b_2-b_1=-\frac{\omega_1}{\omega_0-2\omega}\left[e^{i(\omega_0-2\omega)(T+\tau)}-e^{i(\omega_0-2\omega)T}\right]$$
$$=b_1\,e^{i(\omega_0-2\omega)T}. \tag{10}$$

Thus we find

$$b_2=b_1\left[1+e^{i(\omega_0-2\omega)T}\right]. \tag{11}$$

Since we neglect the damping due to spontaneous emission, $\tilde{b}(t)$ remains equal to b_2 for $t\geqq T+\tau$. From the experimental point of view, if the photomultiplier detecting the fluoresence is gated so that it opens only for $t\geqq T+\tau$, the detected signal then is proportional to $|b_2|^2$.

From (9) we obtain

$$|b_1|^2=\omega_1^2\left[\frac{\sin(\omega_0-2\omega)\tau/2}{(\omega_0-2\omega)/2}\right]^2, \tag{12}$$

where $|b_1|^2$ is the probability of excitation of the atom after the first pulse. Figure 6 shows the plot of $|b_1|^2$ as a function of the laser's angular frequency ω. It is a diffraction curve centered at $\omega=\omega_0/2$ with a width of the order of $2\pi/\tau$, i.e., inversely proportional to the duration τ of a single pulse.

From (11), however, we obtain

$$|b_2|^2=|b_1|^2\,|1+e^{i(\omega_0-2\omega)T}|^2$$
$$=4|b_1|^2\left[\cos\frac{\omega_0-2\omega}{2}T\right]^2. \tag{13}$$

The oscillatory term in (13) corresponds to interference fringes appearing within the diffraction profile $4|b_1|^2$. Figure 7 shows the plot of $|b_2|^2$ as a function of ω. The fringe spacing $\Delta\omega$ is given by the period in ω of the $\{\cos[(\omega_0-2\omega)/2]T\}^2$ term of (13)

$$\Delta\omega=\frac{\pi}{T}. \tag{14}$$

Since $\omega=2\pi\nu$, the fringe spacing is

$$\Delta\nu=\frac{1}{2T}. \tag{15}$$

Substituting $|b_1|^2$ from (12) into (13), we obtain

$$|b_2|^2=4\omega_1^2\tau^2\left[\frac{\sin(\omega_0-2\omega)\tau/2}{(\omega_0-2\omega)\tau/2}\right]^2\left[\cos\frac{\omega_0-2\omega}{2}T\right]^2. \tag{16}$$

Thus $|b_2|^2$ has its maximum value when $\omega=\omega_0/2$. Consequently, if we neglect the light-shifts, the central fringe is *exactly centered* at $\omega=\omega_0/2$. Furthermore, the position of the central fringe does not depend on T, while the spacing between fringes is T dependent. T can fluctuate for various reasons, such as instability or vibration in the optical path; however, any fluctuations in T will not affect the position and amplitude of the central fringe, but will rather produce a decrease in the amplitude of the lateral fringes. Experiments can be performed either by varying ω, with ω_0 and T held fixed, or by varying the Bohr frequency of atomic transition ω_0 (for example, by Zeeman tuning), holding ω and T fixed. Note that, since the central fringe is always exactly centered, small fluctuations of T are not crucial for experiments of this type, as far as spectroscopic applications are concerned. Note also that ω and ω_0 play a symmetric role in our experiment. Of course, one can also vary T, with ω_0 and ω held fixed; such a procedure is discussed later.

Thus far, we have neglected the decay of the excited state populations due to spontaneous emission. This is a good approximation when the delay time T between the two pulses is much less than the radiative lifetime of the excited state, i.e., pulse duration $\tau<T\ll$ radiative lifetime $\tau_R=1/\Gamma$, where Γ is the natural linewidth of the excited state.

However, when T is not shorter than the radiative lifetime of the excited state, one needs to take into account the decay of b_1 by a factor of $\exp(-\Gamma T/2)$ between the first and the second phase-locked pulses. Thus one should replace b_1 by $b_1\exp(-\Gamma T/2)$ in the left-hand side of (10)

$$b_2-b_1\,e^{-\Gamma T/2}=b_1\,e^{i(\omega_0-2\omega)T} \tag{17}$$

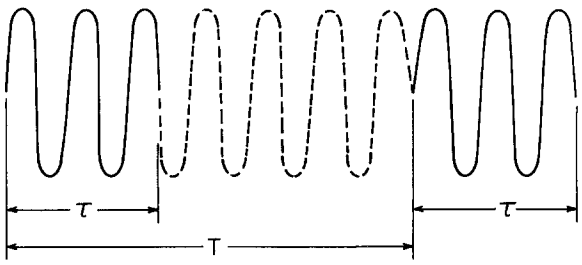

Fig. 8. Pulse pair generated by an optical delay line. Note the difference in phase

or

$$b_2 = b_1[e^{-\Gamma T/2} + e^{i(\omega_0 - 2\omega)T}]. \tag{18}$$

The two terms which interfere in the bracket of (18) no longer have the same modulus, and the contrast of the interference fringes is thus no longer equal to one. When the interference of these two terms is maximum, the square of this bracket takes the value $[1+\exp(-\Gamma T/2]^2$. The minimum value, on the other hand, is equal to $[1-\exp(-\Gamma T/2)]^2$. Thus the contrast of the fringes is

$$C = \frac{(1+e^{-\Gamma T/2})^2 - (1-e^{-\Gamma T/2})^2}{(1+e^{-\Gamma T/2})^2 + (1-e^{-\Gamma T/2})^2} = \frac{2e^{-\Gamma T/2}}{1+e^{-\Gamma T}}. \tag{19}$$

Hence the contrast, which is equal to one for $T \ll 1/\Gamma$, tends to zero when $T \gg 1/\Gamma$. Also note that when $T = 1/\Gamma = \tau_R$, then $c \simeq 0.5$. In other words, increasing the delay between the two pulses causes the fringe spacing and the fringe contrast to decrease; consequently, one obtains better resolution with a smaller signal-to-noise ratio. This can be understood by noting that when $T > \tau_R$, a smaller number of atoms can live for a sufficiently long time to experience the second pulse; since it is interference due to the second pulse that provides the high resolution, only the still-excited atoms contribute to the signal.

Note that in this type of experiment any jitter in cw dye laser frequency will also contribute to a reduction in contrast.

3. Second Possible Experiment

A second possible method of generating a sequence of two phase-locked and Fourier limited pulses, which is experimentally simpler and which we have used, is to start with a Fourier limited pulse (obtained by amplifying a cw wave) and to generate two pulses from it in an optical delay line [7]. The time dependence of the resulting wave has the shape represented by the solid lines of Fig. 8. The second pulse is just the time translation of the first one by an amount T ($T > \tau$). However, the sinusoid extrapolated from the first pulse (dotted lines) generally does not match the second pulse, which means that the two pulses do not have the same phase, unless T is an integral multiple of the optical period $2\pi/2\omega$ [i.e., $\exp(i\omega T) = \pm 1$]. The phase shift appearing in Fig. 8 depends on T, and thus T must remain constant with a good precision, which requires a very stable optical delay line. This situation contrasts with the experiments of Fig. 5 where the fluctuations of T were not critical.

One can write the electric field corresponding to the two pulses of Fig. 8

$$E(t) = \begin{cases} E\,e^{-i(\omega t - \phi)} & \text{for } 0 \leqq t \leqq \tau \\ E\,e^{-i[\omega(t-T)-\phi]} & \text{for } T \leqq t \leqq T+\tau \\ 0 & \text{elsewhere.} \end{cases} \tag{20}$$

Thus the corresponding $\mathscr{D}\mathscr{E}(t)$ is

$$-\mathscr{D}\mathscr{E}(t) = \begin{cases} \omega_1\, e^{-2i\omega t} & \text{for } 0 \leqq t \leqq \tau \\ \omega_1\, e^{-2i\omega(t-T)} & \text{for } T \leqq t \leqq T+\tau \\ 0 & \text{elsewhere.} \end{cases} \tag{21}$$

where

$$\omega_1 \sim E^2.$$

Note that for $0 \leqq t \leqq \tau$, (21) and (4) are identical. Thus, after integrating the Schrödinger equation, the value of b_1 will be the same as that of (9). On the other hand, the value of b_2 is obtained by integrating

$$i\dot{\tilde{b}} = \omega_1\, e^{i\omega_0 t}\, e^{-2i\omega(t-T)} = \omega_1\, e^{i(\omega_0 - 2\omega)t}\, e^{2i\omega T} \tag{22}$$

between T and $T+\tau$, with the initial condition $\tilde{b}(T) = b_1$; thus one obtains

$$b_2 - b_1 = b_1\, e^{i(\omega_0 - 2\omega)T}\, e^{2i\omega T} = b_1\, e^{i\omega_0 T} \tag{23}$$

or

$$b_2 = b_1[1 + e^{i\omega_0 T}]. \tag{24}$$

Therefore,

$$|b_2|^2 = 4|b_1|^2 \cos^2 \frac{\omega_0 T}{2}. \tag{25}$$

Thus one obtains interference fringes within the diffraction profile centered at $\omega_0 = 2\omega$, associated with $|b_1|^2$, with a period

$$\Delta\omega_0 = \frac{2\pi}{T}. \tag{26}$$

Note that in general the central fringe is not centered at $\omega_0 = 2\omega$. Figure 9 shows the variation of $|b_2|^2$ as a function of ω_0, with ω and T held fixed. The dotted line corresponds to the diffraction profile of $|b_1|^2$.

Note that from (25) and (12) we have

$$|b_2|^2 = 4\omega_1^2 \left[\frac{\sin(\omega_0 - 2\omega)\tau/2}{(\omega_0 - 2\omega)/2}\right]^2 \cos^2 \frac{\omega_0 T}{2}$$

$$= 4|b_1|^2 \cos^2 \frac{\omega_0 T}{2}. \tag{27}$$

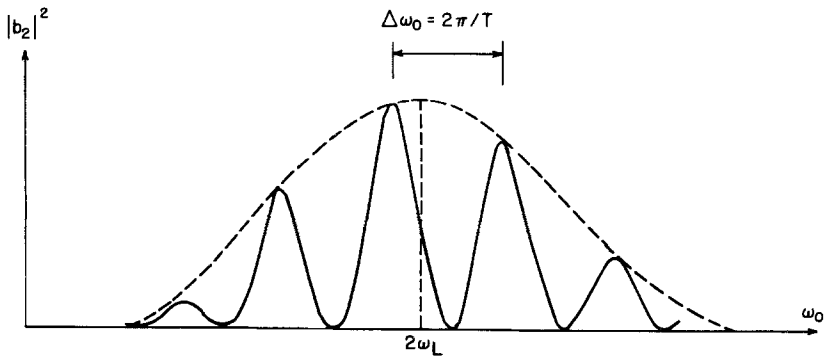

Fig. 9. $|b_2|^2$ as a function of Bohr angular frequency ω_0 of atomic transition

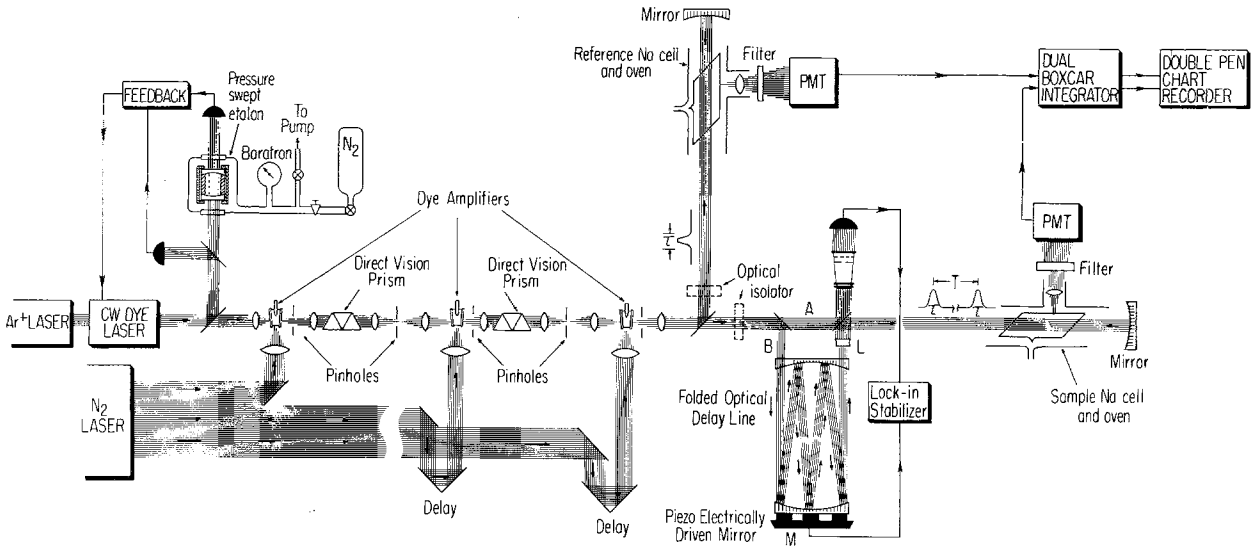

Fig. 10. The experimental arrangement

Therefore, the only variation of $|b_2|^2$ with ω comes from $|b_1|^2$, i.e., from the diffraction profile. Thus if ω is varied, with ω_0 and T held fixed, one does not expect any interference fringes. The difficulty is that when ω varies, the second pulse is dephased by an amount $\exp(i\omega T)$ with respect to the first pulse (see Fig. 8); thus when ω is averaged, the interference fringes will be washed out.

One possible scheme for locking the phases of the two pulses, and consequently causing the interference fringes to reappear centered exactly at $\omega=\omega_0/2$, is to simultaneously vary T when ω is varied in such a way that $\exp(i\omega T)=\pm 1$. Then $\exp(2i\omega T)$, the dephasing factor between the two effective fields for the two-photon resonances in (22), becomes $[\exp(i\omega T)]^2 = [\pm 1]^2 = 1$.

The fact that T varies simultaneously with ω is not important for this experiment, since as we showed in the description of the experiment of Fig. 5, when the two pulses of effective electric field are in phase the central fringe is exactly centered, and small variations of T do not affect it as long as $\exp(2i\omega T)$ remains equal to $+1$.

Furthermore, since we set $\Delta\phi = \nu\Delta T + T\Delta\nu = 0$, so that $\Delta\nu/\nu = -\Delta T/T$ is small (since $\Delta\nu$ is of the order of $1/\tau \sim 50\,\mathrm{MHz} \ll \nu$), the fringe splitting is practically unaffected.

We will describe later how we vary T simultaneously with ω in order to keep $\exp(i\omega T)=\pm 1$ in our experiment.

Figure 10 shows the experimental arrangement [7]. We utilized a single mode cw dye laser (Spectra Physics 580 A, frequency-stabilized to a pressure-tuned reference etalon, and pumped by a Spectra Physics 165 Ar^+ laser) which is tuned to the 3^2S-4^2D two-photon transition in sodium (5787.3 Å). (Note: the lifetime of the 4^2D state is $\sim 5\times 10^{-8}$ s). The output of this cw dye laser (40 mW, 2 MHz) was then amplified in three synchronized stages of dye amplifiers pumped by a one-megawatt nitrogen laser. (Three stages of amplification were necessary to boost the peak output power to an acceptable level for this experiment.) The pump light for the amplifiers was geometrically divided between the amplifiers, and was optically delayed in order to arrive slightly later than the input from the

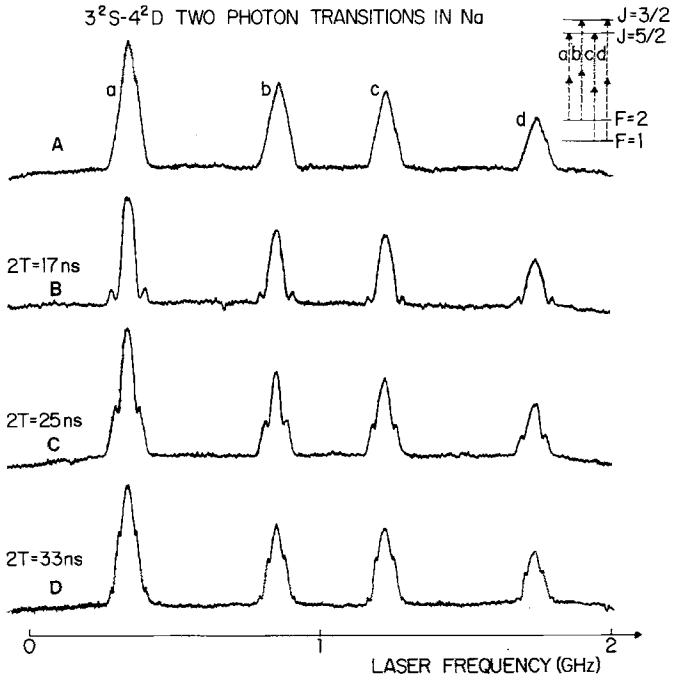

Fig. 11. (a) Recording of the four Doppler free two-photon resonances corresponding to the 3^2S-4^2D transitions of Na (transitions $3^2S_{1/2,3/2}(F=2, F=1)\rightarrow 4^2D_{3/2,5/2}$ observed in the reference cell excited with a single pulse. (b), (c), and (d) Same resonances observed in the sample cell excited with two time-delayed coherent pulses. Width of each pulse, $\tau=8$ ns; effective delay between two pulses $T_{\text{eff}}=2T=17, 25$, and 33 ns, respectively. The spacings between the fringes, $\Delta\nu\approx 60$, 40, and 30 MHz, respectively, are in good agreement with the theoretical prediction $T/2$

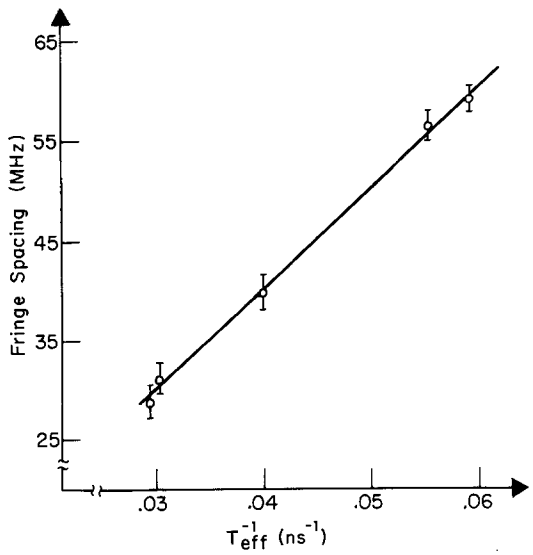

Fig. 12. Splitting between the fringes as a function of T_{eff}^{-1}

evolving pulse building up from the cw dye laser, to maximize the length of the output pulse. To avoid undesirable amplified spontaneous emission from the amplifiers, suitable spectral and spatial filters were inserted between stages. (A detailed description of this oscillator-amplifier dye laser system is presented elsewhere [8].) The 75 kW output of the third stage amplifier was split into two parts, one of which went into a reference sodium cell, and one of which was further split into another two parts. The first of these (Part A in Fig. 10) was sent directly into a sample sodium cell, and the second (Part B in Fig. 10) was optically delayed in a delay line by a time T ($2T=17$, 25, 33 nanoseconds), and subsequently recombined with the first and focused into the sample sodium cell. We stabilized the delay line by locking the center fringe of the two cw carrier beams (which is at maximum when the direct and the delayed cw carrier beams are in phase, i.e., when $\exp(i\omega T)=1$) to the motion of the mirror M, which was mounted on a piezo-electric ceramic. In this way, the two time-delayed and Fourier-limited pulses were phase-locked during the entire experiment. Furthermore, the delayed beam, with its longer optical path, had wavefronts with a larger radius of curvature than those of the direct beam, so a high quality lens (L) was used to match the curvature of the two wavefronts. Both sodium cells were kept at 130° C (2×10^{-6} Torr of vapor pressure); they were made of Corning 1720 calcium aluminosilicate glass with optically flat windows and were baked at high temperature and later filled with sodium under very high vacuum to avoid any foreign gas contamination. To generate the laser standing waves with short pulses, the back reflecting mirror was adjusted so that the time delay between the original pulse and the back reflected pulse was significantly shorter than the pulse duration τ. The outputs of the two photomultipliers (EMI 9635 QB) monitoring the fluorescence from $4P$ to $3S$ at 3303 Å were simultaneously processed by a dual channel boxcar integrator, whose 100 ns wide gates were independently triggered after the delayed pulse (for the sample cell) and after the original pulse (for the reference cell). The results were recorded simultaneously by a dual pen chart recorder.

Figure 11a shows the four well-known two-photon resonances of the 3^2S-4^2D transition of Na, observed in the reference cell with a single pulse. Figure 11b shows the same four resonances observed in the sample cell which is excited by the two time-delayed coherent pulses with $2T\simeq 17$ ns. An interference structure clearly appears on each resonance. Figure 11c and d show the same experimental traces as those of Fig. 11b except for effective delays of $T_{\text{eff}}=2T=25$ and 33 ns, respectively. Note that in these cases (Fig. 11c and d) the contrast of the fringes is progressively less than that of Fig. 11b, where a shorter delay is used. We have verified that with the delay line unlocked the interference fringes disappear (when ω is varied). Figure 12 shows a plot of the splitting between the fringes as a function of T_{eff}^{-1}, where $T_{\text{eff}}=2T$ is the effective delay time between the two phase-locked pulses. The error bars are due largely to

statistical errors and to the precision involved in measuring the exact fringe splittings, which were calibrated by the known fine structure of the 4^2D excited state and hyperfine structure of the 3^2S ground state in the upper trace.

Clearly, it is possible to choose T longer than the radiative lifetime of the excited state, in which case the resolution would be better than the natural linewidth. In such a case, however, only those atoms that remain in the excited state for a time at least equal to T would contribute to the interference effect, and consequently the fringes would have a very poor contrast. This can be understood analytically from the influence of the radiative lifetime of the excited states, (19), since by increasing T one obtains a better resolution (i.e., fringe spacing decreases) accompanied by a smaller contrast, and consequently a smaller signal-to-noise ratio.

4. Elimination of Diffraction Background

Going back to the discussion of Fig. 2, the sum of the two quantum mechanical amplitudes A_1 and A_2 represents the total amplitude $A=A_1+A_2$ for reaching the excited state $|e\rangle$ from the ground state $|g\rangle$. When one introduces a phase shift $\exp(i\delta)$ on the second pulse only, then the total amplitude is $A_1+\exp(i\delta)A_2$, and the probability of reaching the $|e\rangle$ state is

$$|A|^2=|A_1+e^{i\delta}A_2|^2=\underbrace{|A_1|^2+|A_2|^2}_{\substack{\text{diffraction}\\ \text{terms}}}+\underbrace{2A_1A_2\cos\delta}_{\substack{\text{interference}\\ \text{terms}}}.$$

In order to eliminate the diffraction background appearing in each of the four resonances of Fig. 11b, c, and d, one could induce a 90° phase shift (so that $\delta=180°$ for the two-photon excitation) between every other pair of coherent pulses into the sample cell. By subtracting the resulting fluorescence from pairs of coherent pulses with and without the phase shift:

$$|A|^2_{\delta=0}-|A|^2_{\delta=\pi}=4A_1A_2$$

one can eliminate the diffraction background and thus isolate the interference fringes. Note that in this way not only does one get rid of the diffraction background, but also one doubles the interference signal automatically.

Thus when the contrast is not equal to one, it is possible to eliminate the diffraction background in order to isolate the interference fringes [8]. One can introduce a phase shift on the second pulse of Fig. 1c by, for example, sending the two pulses through a crystal plate and applying an electric field to the plate immediately after the first pulse has passed through, so that the index of refraction changes *for the second pulse only*. If $\exp(i\delta)$ is the phase shift for the second pulse, then [4] will become

$$-\mathscr{D}\mathscr{E}(t)=\begin{cases}\omega_1 e^{-2i\omega t} & \text{for } 0\leqq t\leqq\tau\\ \omega_1 e^{-2i(\omega t-\delta)} & \text{for } T\leqq t\leqq T+\tau\\ 0 & \text{elsewhere}\end{cases}\qquad(4')$$

where

$$\omega_1\sim E^2.\qquad(5')$$

Note that in (9), b_1 does not change, but b_2-b_1 is multiplied by $\exp(2i\delta)$ in (10), so that (11) becomes

$$b_2=b_1[1+e^{i[(\omega_0-2\omega)T+2\delta]}].$$

Note also that ω and T are locked together so that $\exp(i\omega T)=\pm1$; hence (11) and (24) are equivalent, and the former shows the structure more clearly. Thus

$$|b_2|^2=4|b_1|^2\left[\cos\frac{(\omega_0-2\omega)T+2\delta}{2}\right]^2.\qquad(28)$$

This produces a shift δ/T of the whole interference structure within the diffraction profile. If δ is chosen equal to $\pi/2$ (by applying the proper voltage to the crystal), then the shift corresponds to half a fringe spacing. By subtracting the signals corresponding to $\delta=0$ and $\delta=\pi/2$, one obtains

$$\begin{aligned}&|b_2(\delta=0)|^2-|b_2\left(\delta=\frac{\pi}{2}\right)|^2\\&=4|b_1|^2\left[\cos^2\frac{(\omega_0-2\omega)T}{2}-\sin^2\frac{(\omega_0-2\omega)T}{2}\right]\\&=4|b_1|^2\left[2\cos^2\frac{(\omega_0-2\omega)T}{2}-1\right].\end{aligned}\qquad(29)$$

Thus not only is the diffraction background suppressed, but the interference signal is automatically doubled. Note that it remains centered at $\omega=\omega_0/2$.

Figure 13 shows our experimental setup. It is identical to the arrangement of Fig. 10, except that the N_2 laser was externally triggered by a homemade trigger generator. The trigger generator produced a train of pulses. For simplicity, let us distinguish between the first and the second pulses by calling the first pulse A and the second pulse B. Thus, the train of pulses from the trigger generator consisted of a train of A, B pulses. (A and B pulses were each 8 ns long, 50 ms apart).

While a train of AB pulses triggered the N_2 laser, a flip-flop counter discriminated A pulses from B pulses, and after a proper delay the A pulses triggered boxcar I, and the B pulses triggered boxcar II. Since each A pulse and each B pulse from the dye laser gave rise to a pair of A and a pair of B pulses at the sodium sample cell, the electronic delay was adjusted so that the 100 ns wide gates of both boxcars were opened immediately after the delayed pulses, as illustrated in Fig. 14. Meanwhile,

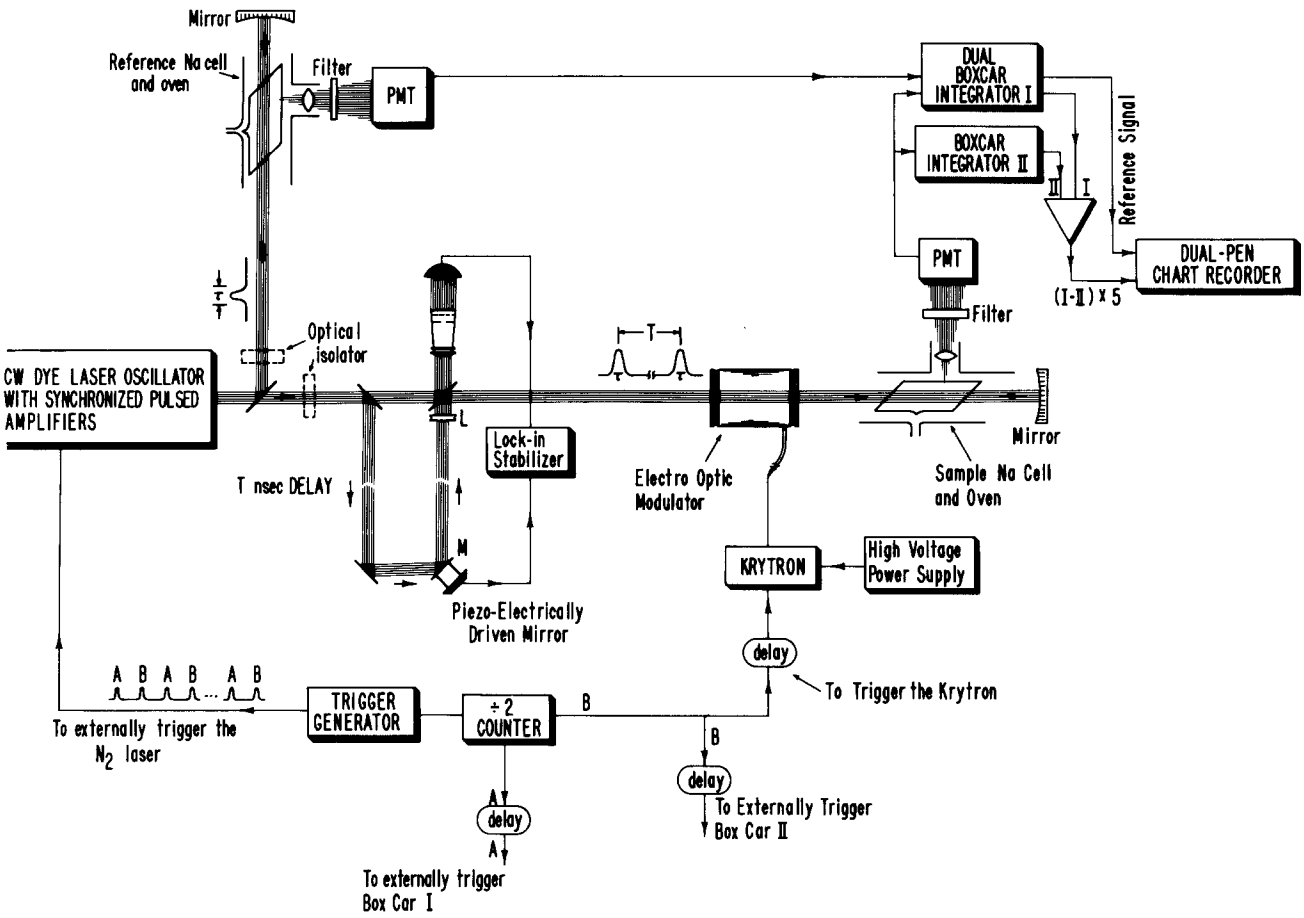

Fig. 13. The experimental setup

the B pulses triggered an EG&G KN-22 Kryton switch which turned on a Pockels cell (Interactive Radiation Model 212-080, or Isomet Model EON 4203). The voltage on the Pockels cell was adjusted so that it would produce a 90° phase shift on the delayed B pulses; moreover, the Krytron switch turned on slightly ahead of the delayed B pulses and turned off slightly after the delayed B pulses, as illustrated in Fig. 14. For this reason, proper care had to be taken in the design of the trigger generator so that the Pockels cell remained on before and after the delayed B pulses to allow for any possible jitter associated with the rise time of the KN-22 Krytron and the Pockels cell. The outputs of the two boxcar integrators were subtracted in a linear differential amplifier and the result was recorded on a chart recorder.

The reference sodium cell used in our experiment allowed us not only to calibrate the frequency accurately (since the cw oscillator was frequency-stabilized to a pressure-tuned reference etalon), but also to examine the elimination of the diffraction background as a result of the 90° phase shift between B pulses. The output of the reference PMT (EMI-9635 QB) monitoring the resulting $4P \rightarrow 3S$ fluorescence at 3302 Å due to single pulse excitation (train of AB pulses) was processed by the other channel of the PAR 162 boxcar integrator, whose gate was triggered just after the A and B pulses, and the resulting fluorescence was recorded by the same dual pen chart recorder.

Figure 15b shows the experimental results for a delay of 25 ns. Above it, Fig. 15a corresponds to the reference sodium cell. A number of important tests were performed to assure that these data corresponded to real isolated Ramsey fringes. First, it was verified that no signal was observed when zero phase shift was introduced between B pulses (by turning off the high voltage supply to the Krytron). Figure 15c shows this result. (An equivalent test would have been to induce a 180° phase shift between B pulses, in which case one again expects a null signal. However, the electronic circuitry for triggering the Krytron did not allow us to increase the voltage enough to provide a 180° phase shift. A slight modification in the electronic design should make this test also possible.) Second, by slightly varying the voltage supplied to the electro-optic modulator, and thus in effect slightly varying the phase of the phase-shifted delayed B pulses, the signal was opti-

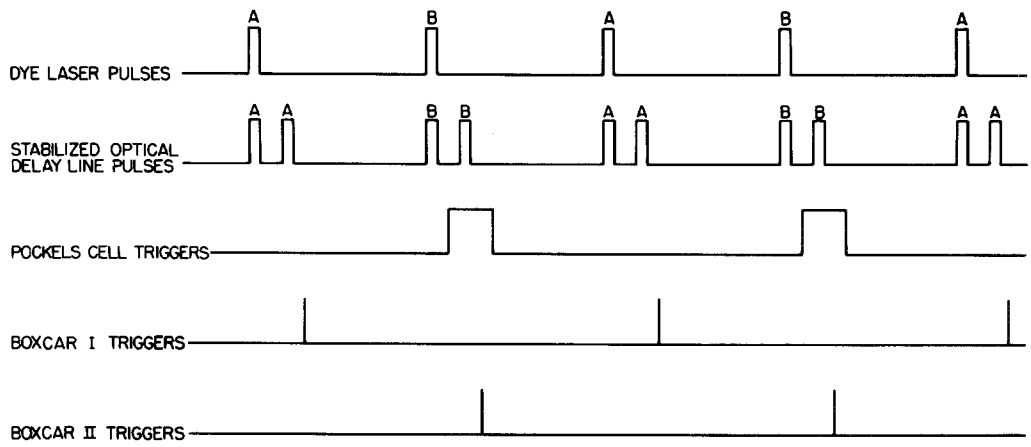

Fig. 14. The timing sequence of the electronic triggering system for triggering the Pockels cell, boxcar I, and boxcar II

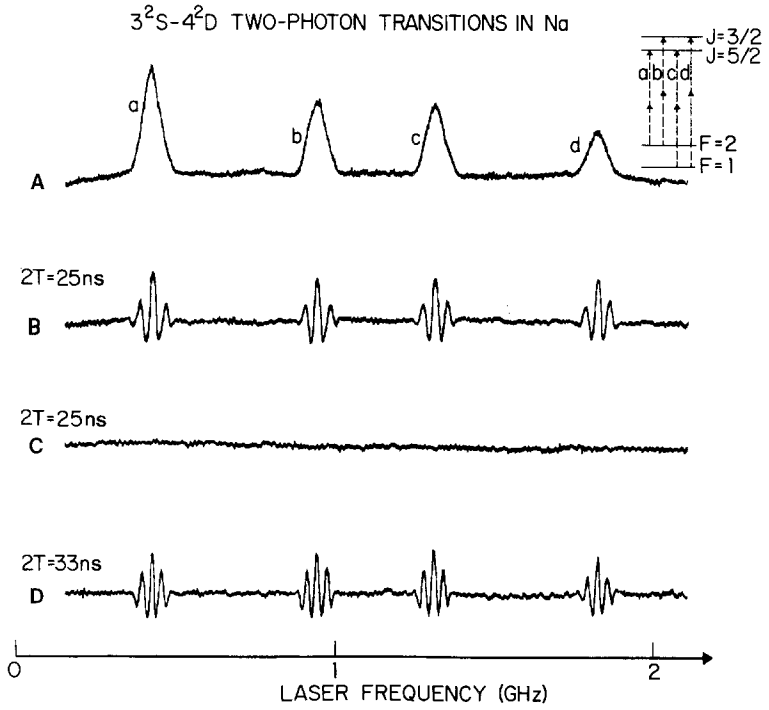

Fig. 15. (a) The four Doppler-free 3^2S-4^2D two-photon resonances of Na observed in the reference cell excited with a single pulse of $\tau=8$ ns duration, (b) and (d) The same resonances observed in the sample cell excited with two time-delayed coherent pulses (with $2T=25$ ns and $2T=33$ ns, respectively), where a 90° phase shift is introduced between alternate pairs of pulses, and with amplification of the difference between the fluorescence resulting from pairs of coherent pulses with and without the phase shift. (c) The same resonances and procedure as for Fig. 3b except that zero phase shift is introduced between alternate pairs of coherent pulses

mized, so that at the voltage corresponding to the exact 90° phase shift the diffraction background was completely eliminated. There was still some small background in some of the experimental traces which could be eliminated only by making a slight adjustment in the Krytron power supply voltage. This was attributed to the induced phase jitter associated with the electro-optic modulator; the pulse-to-pulse jitter in the phase shift induced by the Pockels cell may have been the source of this difficulty.

Figure 15d shows similar experimental results for a delay of 33 ns. Note that in this case the fringe spacings are much smaller than in the case of $T_{\text{eff}}=25$ ns delay. Again it was verified that the fringe spacing was proportional to T_{eff}^{-1}. In comparison with Figs. 11c and d, note the enormous gain in contrast associated with the traces of Figs. 15b and 15d.

5. Extension to Longer Delays

Clearly, using this technique of phase modulation between alternate coherent pulse pairs, it should be possible to achieve a resolution much smaller than the natural linewidth of the excited state. The condition for this possibility is

$$\text{(Fringe spacing)} = \frac{1}{T_{\text{eff}}} = \frac{1}{2T} < \frac{1}{2\pi\tau_R} = \text{(Natural linewidth of the excited state)} \tag{30}$$

or

$$T_{\text{eff}} = 2T > 2\pi\tau_R . \tag{31}$$

Thus the effective delay between the two pulses must be longer than the radiative lifetime of the excited state multiplied by 2π.

For the case of the 4^2D excited state, $\tau_R \simeq 50$ ns. Thus

$$2T > 2\pi \times 50\,\text{ns}$$

or

$$T > 160\,\text{ns}.$$

In order to obtain such a delay, one needs an ultra-stable delay line with mirrors of ultra-high optical quality, so that locking the center fringe of the two cw beams (direct and delayed) to the motion of the piezoelectrically driven mirror would become less troublesome. Also for such a long delay the wavefront curvature might be a serious problem; we have observed that when the wavefronts are not mode-matched, the contrast of the fringes is reduced, and some asymmetry of the side fringes relative to the position of the central fringe develops. However, it is conceivable that all these difficulties could be overcome with a reasonable amount of effort. A more sophisticated detection system is needed, however, since the signal from the small number of longer lived atoms might be hopelessly buried in laser fluctuations and detector noise.

Since our laser source is repetitively pulsed and the fluorescent decay photons necessarily appear within a few microseconds of the laser pulse, the output of the photodetector is averaged by a gated integrator system which accepts signals during limited time intervals. This technique eliminated most of the photomultiplier background without the need for cooling the detector, and eliminated as well spurious signals due to overhead lights and the cw oscillating waves which were collinear with the pulses. Theoretically, the minimum detectable signal is then on the order of one photoelectron per laser pulse. In real experimental situations, however, various phenomena degrade the signal-to-noise ratio obtained by this method, making it impossible to observe the interference fringes. For instance, at the low signal levels involved, all materials fluoresce somewhat when excited by a laser, and care must be taken to shield the photodetector from such spurious radiation. Furthermore, undesirable fluorescence may result from linear absorption in the sample itself. Another problem is that many alkali metal vapors, for example, can form dimers capable of absorbing the frequencies needed for two quantum absorption in the atoms. Many of the excited molecules will then decay by fluorescing at wavelengths longer than the incident wavelength. However, some molecules may absorb a second quantum and dissociate into atoms, one of which may be significantly excited to radiate at an atomic line of wavelength shorter than the incident radiation.

If the detected fluorescence corresponds to a resonance line (as in our case for the detection of $4^2P - 3^2S$ at 3302 Å), the phenomenon of self-absorption will result in the occurrence of the bulk of the fluorescence signal on the resonance line of longest wavelength, in violation of the expected branching ratios. Finally, one might encounter a situation in which ac Stark effect would wash out the interference signal. For example, when an accidental near-resonant or resonant enhancement is encountered the pulse-to-pulse jitter can give rise to a random ac Stark shift from one pulse to the other. This could easily bury the interference signal for these long-lived atomic states.

All other techniques having failed, it is indeed possible to detect the interference signal on a single quantum event basis by interfacing the signal with an on-line computer, thus accumulating and averaging the data over a long period of data taking.

Conclusion

In this paper we have introduced a technique which could mark the beginning of a new epoch in optical physics, where through the use of delayed pulses, pulse-length broadening can be overcome. Thus pulsed dye lasers—the only spectroscopic tool presently available in many spectral regions—can be used for ultrahigh-resolution spectroscopy of atomic and molecular systems. This work marks a logical beginning to a stimulating and exciting new generation of optical experiments. Our technique can be generalized; instead of two pulses, one could use a sequence of N equally spaced pulses (obtained, for example, by sending an initial pulse into a confocal resonator [9]), and thus submit atoms to a series of N equally spaced time-delayed and phase-locked pulsed standing waves. Such narrow multipulse resonance lines have recently been observed by Teets et al. for the $3^2S - 5^2S$ two-photon transitions of sodium [10]. An argument parallel to the discussion of Fig. 1 would show that the optical analogue of such a system is a grating with N lines; the total length of the grating corresponds to the total duration NT of the pulse train. In such a case, the frequency spectrum experienced by the atom would be a series of narrow peaks, N times narrower in width and N^2 times stronger in intensity, separated by a frequency interval T_{eff}^{-1}.

Acknowledgement. I am deeply indebted to Professor C. Cohen-Tannoudji for much invaluable advice and constant enthusiasm for this work. I also wish to thank Professor N. Bloembergen for his interest and support of this work; Dr. J. Vigué and my other colleagues at Ecole-Normale Supérieure (Paris) for many con-

structive suggestions and criticisms. Thanks are also due to P. H. Cox, L. Donaldson, R. W. Stanley, D. A. Van Baak, and S. S. Mertz for expert technical assistance and help in data taking.

References

1. L.S.Vasilenko, V.P.Chebotayev, A.V.Shishaev: Pis'ma Zh. Eksp. Teor. Fiz. **12**, 161 (1970) [JETP Lett. **12**, 113 (1970)];
B.Cagnac, G.Grynberg, F.Biraben: J. Phys. (Paris) **34**, 56 (1973) and Phys. Rev. Lett. **32**, 643—643 (1974);
M.D.Levenson, N.Bloembergen: Phys. Rev. Lett. **32**, 645 (1974);
T.W.Hänsch, K.Harvey, G.Meisel, A.L.Schawlow: Opt. Comm. **11**, 50 (1974);
M.M.Salour: Opt. Comm. **18**, 377 (1976);
J.P.Woerdman: Chem. Phys. Lett. **43**, 279 (1976)
For a review see N.Bloembergen, M.D.Levenson, in: *High-Resolution Laser Spectroscopy*, ed. by K.Shimoda, Topics Appl. Phys., Vol. 13 (Springer Berlin, Heidelberg, New York 1976)
2. M.M.Salour: Opt. Comm. **18**, 377 (1976);
M.M.Salour, Ph.D. thesis, Harvard University (1977)
3. N.F.Ramsey: Phys. Rev. **76**, 996 (1949); and *Molecular Beams* (Oxford University Press: New York 1956);
P.B.Kramer, S.R.Lundeen, B.O.Clark, F.M.Pipkin: Phys. Rev. Lett **32**, 635 (1974)
4. Ye.V.Baklanov, B.Ya.Dubetskii, V.P.Chebotayev: Appl. Phys. **9**, 171 (1976); and Appl. Phys. **11**, 201 (1976);
B.Ya.Dubetskii: Kvantovaya Elektron. (Moscow) **3**, 1258 (1976) [Sov. J. Quantum Electron. **6**, 682 (1976)]
5. J.C.Bergquist, S.A.Lee, J.L.Hall: Phys. Rev. Lett. **38**, 159 (1977)
6. Note that the method of using two coherent time-delayed electromagnetic pulses has already been used in the microwave domain. See, for example: C.O.Alley, in *Quantum Electronics, A Symposium* (Columbia University Press: New York 1960), p. 146; M.Arditi, T.R.Carber: IEEE Trans. IM-13, 146 (1964)
7. M.M.Salour: Bull. Am. Phys. Soc., **21**, 1245 (1976);
M.M.Salour, C.Cohen-Tannoudji: Phys. Rev. Lett. **38**, 757 (1977)
8. M.M.Salour: Opt. Comm. **22**, 202 (1977)
9. M.M.Salour: Appl. Phys. Lett. **31**, 394 (1977)
10. R.Teets, J.Eckstein, T.W.Hänsch: Phys. Rev. Lett. **38**, 760 (1977)
11. F.P.Schäfer (ed.): *Dye Lasers* 2nd ed., Topics Appl. Phys. Vol. 1 (Springer Berlin, Heidelberg, New York 1977)
12. S.L.Shapiro (ed.): *Ultrashort Light Pulses*, Topics Appl. Phys., Vol. 18 (Springer Berlin, Heidelberg, New York 1977)